

## QUANTUM PROPERTIES IN TRANSPORT THROUGH NANOSCOPIC RINGS: CHARGE-SPIN SEPARATION AND INTERFERENCE EFFECTS

K. HALLBERG

*Instituto Balseiro and Centro Atómico Bariloche, CNEA, CONICET,  
8400 Bariloche, Argentina  
karen@cab.cnea.gov.ar*

JULIAN RINCON

*Instituto Balseiro and Centro Atómico Bariloche, CNEA, CONICET,  
8400 Bariloche, Argentina*

S. RAMASESHA

*Solid State and Structural Chemistry Unit, Indian Institute of Science,  
Bangalore 560 012, India*

Received 2 December 2009

Many of the most intriguing quantum effects are observed or could be measured in transport experiments through nanoscopic systems such as quantum dots, wires and rings formed by large molecules or arrays of quantum dots. In particular, the separation of charge and spin degrees of freedom and interference effects have important consequences in the conductivity through these systems.

Charge-spin separation was predicted theoretically in one-dimensional strongly interacting systems (Luttinger liquids) and, although observed indirectly in several materials formed by chains of correlated electrons, it still lacks direct observation. We present results on transport properties through Aharonov-Bohm rings (pierced by a magnetic flux) with one or more channels represented by paradigmatic strongly-correlated models. For a wide range of parameters we observe characteristic dips in the conductance as a function of magnetic flux which are a signature of spin and charge separation.

Interference effects could also be controlled in certain molecules and interesting properties could be observed. We analyze transport properties of conjugated molecules, benzene in particular, and find that the conductance depends on the lead configuration. In molecules with translational symmetry, the conductance can be controlled by breaking or restoring this symmetry, e.g. by the application of a local external potential.

These results open the possibility of observing these peculiar physical properties in anisotropic ladder systems and in real nanoscopic and molecular devices.

*Keywords:* Charge-spin separation; quantum interference; strong correlations.

## 1. Introduction

New artificial structures made using nanotechnology allow for the possibility of tailoring systems with novel physical properties. For example, the Kondo effect was achieved in a system consisting of one quantum dot (QD) connected to leads;<sup>1-3</sup> systems of a few QD's have been proposed theoretically as realizations of the two-channel Kondo model,<sup>4,5</sup> the ionic Hubbard model,<sup>6</sup> and the double exchange mechanism.<sup>7</sup> Also, the correlation-driven metal-insulator transition has been studied in a chain of QD's.<sup>8</sup>

In addition, molecular systems also pose a challenging scenario as seen from various successful attempts.<sup>9-11</sup> The possibility of achieving controlled quantum transport has been studied, for example in electronic conductance through single  $\pi$ -conjugated molecules using theoretical<sup>12-16</sup> and experimental<sup>17-20</sup> techniques.

Several interesting properties arise from these artificial and molecular systems. On one hand, artificial nanorings of nanoladders with strong interacting electrons could be assembled to observe the elusive property of charge-spin separation (SCS), characteristic of strongly correlated low-dimensional systems. Among the theoretical methods for detecting and visualizing SCS, direct calculations of the real-time evolution of electronic wave packets in finite Hubbard rings revealed different velocities in the dispersion of spin and charge densities as an immediate consequence of SCS.<sup>21</sup> Also, Kollath and coworkers<sup>22</sup> have repeated this calculation for larger systems using the Density Matrix Renormalization Group (DMRG) technique<sup>23</sup> and observed distinct features of SCS in a model for one-dimensional cold Fermi gases in a harmonic trap, proposing quantitative estimates for an experimental observation of SCS in an array of atomic wires.

Other calculations were done in Refs. 24 and 25, where the authors analyzed the transmission through infinite Aharonov-Bohm (AB) rings. The motion of the electrons in the ring was described by a Luttinger liquid (LL) propagator with different charge and spin velocities,  $v_c$  and  $v_s$ , included explicitly. With this assumption the flux-dependence of the transmission has, in addition to the periodicity in multiples of the flux quantum  $\Phi_0 = hc/e$ , new structures which appear at fractional values of the flux. Numerical calculations of the transmittance through finite AB rings described by the  $t - J$  and Hubbard models show clear dips at the fluxes that correspond to Eq. (4).<sup>26-29</sup> The extension of these results to ladders of two legs was also considered, as a first step to higher dimensions.<sup>30</sup> In essence, these structures arise because transmission requires the separated spin and charge degrees of freedom of an injected electron to recombine at the drain lead after traveling through the ring in the presence of the AB flux. In this work we will review these results for rings and ladder rings.

On the other hand, quantum interference might play a crucial role in transport measurement through molecules and could be used as a handle to control conductance through such systems. In two recent theoretical works,<sup>14,15</sup> the idea of a Quantum Interference Effect Transistor (QuIET) based on single annulene

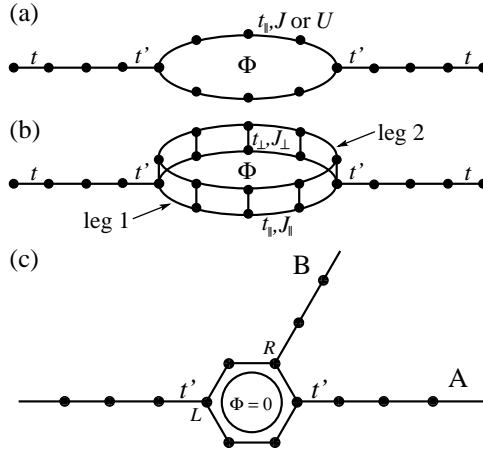


Fig. 1. Schematic representation of the systems considered for electronic transport. a) An interacting ring modelled by the  $t - J$  and Hubbard Hamiltonians; b) a ladder ring represented by the  $t - J$  model and c) conjugated molecules with different number of Carbon atoms and two different lead configurations.

molecules, including benzene, was proposed. The equilibrium conductance at zero bias and gate voltage ( $V_g$ ) was calculated in both papers for the strong coupling limit using the non-equilibrium Green's function and the Landauer-Büttiker formalism. However, annulenes have a gap at the energy corresponding to  $V_g = 0$  due mainly to the strong Coulomb interactions present in the molecule ( $N = 4n + 2$  annulenes like benzene, are closed-shell molecules with no level at zero energy even in the absence of interactions). For zero gate voltage the conductance is finite, albeit small, only for strong coupling to the leads. For weak coupling the conductance will be appreciable only through the main channels of the molecule which are a few eV away from the Fermi energy. By analyzing the QUIET at the main transmittance channels the switching effect will be much more pronounced and robust as we will show below.

In this paper we will show results for the conductance through the three systems depicted in Fig. 1: a) an interacting ring, b) an interacting ladder ring and c) conjugated molecules.

## 2. The Method

Before introducing the models we will describe the method used for the calculation of the transmittance.

The systems considered are sketched in Fig. 1. They consist of interacting rings weakly coupled to two non-interacting leads. Our model Hamiltonian reads  $H = H_{\text{leads}} + H_{\text{link}} + H_{\text{ring}}$ , where  $H_{\text{leads}}$  describes free electrons in the left and right

leads,

$$H_{\text{link}} = -t' \sum_{\sigma} (a_{-1,\sigma}^{\dagger} c_{L,\sigma} + a_{1,\sigma}^{\dagger} c_{R,\sigma} + \text{H.c.}) \quad (1)$$

describes the exchange of quasiparticles between the leads ( $a_{i,\sigma}$ ) and particular sites of the ring, and  $H_{\text{ring}}$  depends on the modelling of the ring.

Following Ref. 24, the transmission from the left to the right lead can be calculated to second order in  $t'$  where the ring is integrated out. The resulting effective Hamiltonian is equivalent to a one-particle model for a non-interacting chain with two central sites modified by the interacting ring, with effective on-site energy  $\epsilon(\omega) = t'^2 G_{L,L}^R(\omega)$  and effective hopping between them  $\tilde{t}(\omega) = t'^2 G_{L,R}^R(\omega)$ .  $G_{i,j}^R(\omega)$  denotes the Green's function of the isolated ring.

The transmittance and conductance of the system at zero temperature may then be computed using the effective impurity problem. The transmittance  $T(\omega)$  is given by<sup>24</sup>

$$T(\omega, V_g, \phi) = \frac{4t^2 \sin^2 k |\tilde{t}(\omega)|^2}{|[\omega - \epsilon(\omega) + te^{ik}]^2 - |\tilde{t}(\omega)|^2|}, \quad (2)$$

where  $\omega = -2t \cos k$  is the tight-binding dispersion relation for the free electrons in the leads which are incident upon the impurities. These equations are exact for a non-interacting system.

From Eq. (2),  $T(\omega, V_g, \phi)$  may be calculated from the Green functions of the isolated ring. We consider holes incident on a ring of  $L'$  sites and  $N = N_e + 1$  electrons in the ground state, obtaining the Green functions from the ground state of the ring modelled by Eqs. (3), (5) and (6) below, and calculated using numerical diagonalization<sup>31</sup> Then we substitute these in Eq. (2). We fix the energy  $\omega = 0$  to represent half-filled leads and explore the dependence of the transmittance on the threading flux, obtained by integration over the excitations in a small energy window, which accounts for possible voltage fluctuations and temperature effects.<sup>26</sup>

### 3. Charge-spin Separation

#### 3.1. Conductance through rings

In this section we will calculate the transmittance through a ring (Fig. 1a) for which the Hamiltonian reads:

$$H_{\text{ring}} = -eV_g \sum_{l,\sigma} c_{l,\sigma}^{\dagger} c_{l,\sigma} - t_{\parallel} \sum_{l,\sigma} (c_{l,\sigma}^{\dagger} c_{l+1,\sigma} e^{-i\phi/L'} + \text{H.c.}) + H_{\text{int}}. \quad (3)$$

where the flux is given in units of the flux quantum  $\phi = 2\pi\Phi/\Phi_0$  and the system is subjected to an applied gate voltage  $V_g$ .

For the Hubbard model  $H_{\text{int}} = \sum_{l,\sigma \neq \sigma'} U n_{l,\sigma} n_{l,\sigma'}$ , with  $n_{l,\sigma} = c_{l,\sigma}^{\dagger} c_{l,\sigma}$ . This model is related to the also well known  $t - J$  model for very large interactions by  $J = 4t_{\parallel}^2/U$  where a similar behaviour to the one described below is also found.<sup>27</sup>

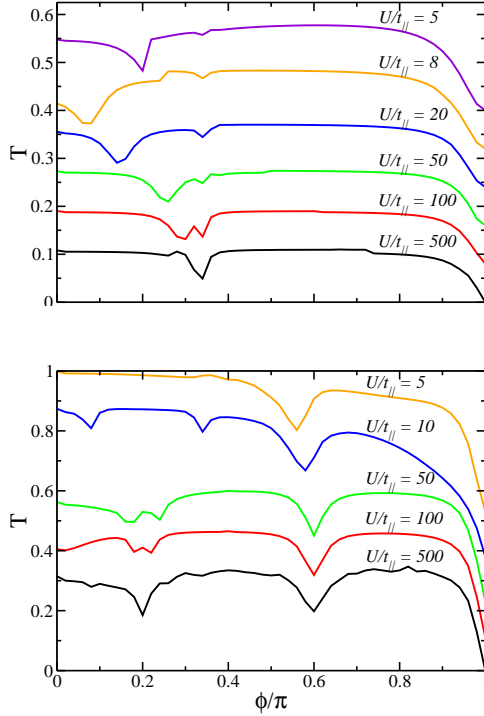


Fig. 2. Transmittance vs flux for the Hubbard model in the 1D ring for  $L = 6$  sites, and a)  $N_e + 1 = 4$  and b)  $N_e + 1 = 6$  particles in the ground state and several values of  $U$  (curves are shifted vertically for better visualization).

In the case of infinite on-site repulsion  $U$  (or equivalently  $J = 0$ ), the wave function can be factorized into a spin and a charge part.<sup>26,32,33</sup> Therefore, charge-spin separation becomes evident for finite systems and independent of system size. For each spin state, the system can be mapped into a spinless model with an effective flux which depends on the spin. Considering a non-degenerate ground state containing  $N = N_e + 1$  particles and analyzing the part of the Green function that enters the transmittance when a particle is destroyed, it is shown that the dips occur when two intermediate states cross at a given flux and interfere destructively. These particular fluxes depend on the spin quantum numbers and are located at<sup>27</sup>

$$\phi_d = \pi(2n + 1)/N_e, \quad (4)$$

with  $n$  integer. If the integration energy window includes these levels, a dip in the conductance arises.

In Fig. 2 we show results for the transmittance using the Hubbard model in the ring. For large interactions,  $U \gg t_{\parallel}$ , dips are found at the positions given by Eq. (4). However, when  $U$  is reduced increasing the mixture between different spin

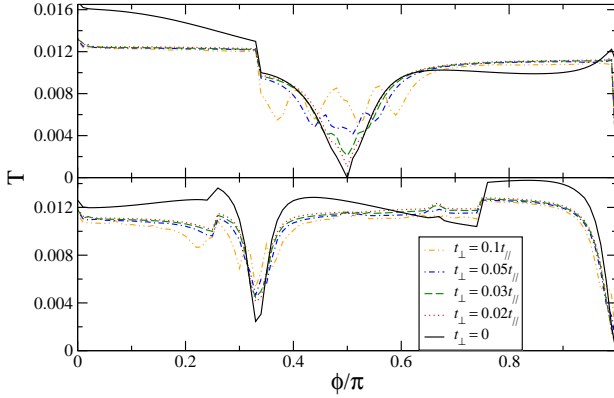


Fig. 3. Flux-dependent transmittance for the anisotropic  $t-J$  model with  $J = 0$ ,  $t_{\parallel} = 0.1$ ,  $L = 6$  rungs,  $t' = 0.05t_{\parallel}$ , several values of  $t_{\perp}$  and  $N = 6$  (top) and  $N = 8$  (bottom) electrons in the ground state.

sectors, the spin-charge separation is affected and we observe the appearance of new dips and a shift of some of them. This is because the destructively interfering level crossings which lead to the reduction in the conductance occur at different values of the flux, as explained in Ref. 27.

### 3.2. Conductance through ladder rings

In this subsection we analyze the conductance through rings formed by two-leg ladder systems described by the  $t-J$  model as a first step towards two dimensions (Fig. 1b). For this case the Hamiltonian of the interacting system reads:

$$\begin{aligned}
 H_{\text{ring}} = & -eV_g \sum_{i,l,\sigma} c_{i_l,\sigma}^{\dagger} c_{i_l,\sigma} - t_{\parallel} \sum_{i,\sigma} (c_{i_l,\sigma}^{\dagger} c_{i_{l+1},\sigma} e^{-i\phi/L'} + \text{H.c.}) \\
 & - t_{\perp} \sum_{i,\sigma} (c_{i_1,\sigma}^{\dagger} c_{i_2,\sigma} + \text{H.c.}) + H_{\text{int}}
 \end{aligned} \quad (5)$$

The fermionic operators  $c_{i_l,\sigma}^{\dagger}$  create an electron at site  $i = 1, L'$  of leg  $l = 1, 2$  with spin  $\sigma$ . The AB ring has  $L'$  rungs, is threaded by a flux  $\phi$  ( $\phi = 2\pi\Phi/\Phi_0$ ), and is subjected to an applied gate voltage  $V_g$ .

We first show results for weakly coupled chains ( $t_{\perp} \ll t_{\parallel}$ ) and  $J = 0$ , where we know that in 1D there is complete SCS.<sup>26,32,33</sup> In Fig. 3 we show the results for several small values of  $t_{\perp}$  and in fact, observe clear dips at certain fractional values of the magnetic flux.

To understand the position of the dips for this case of weakly coupled rings we must consider the following: For the ladder with  $t_{\perp} = 0$  and a total even number of electrons  $N$  in the ground state, the lowest-lying state has  $N/2$  electrons in each leg. Since we are calculating the transmittance through one leg only, and the

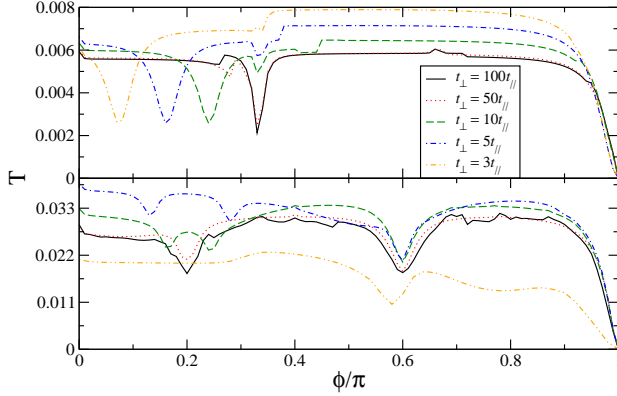


Fig. 4. Transmittance as a function of flux for  $J = 0$ . Top:  $t' = 0.05t_{\parallel}$  and  $N = 4$  electrons. Bottom:  $t' = 0.09t_{\parallel}$  and  $N = 6$  electrons.

intermediate state has one particle less, one expects to see dips at  $\phi_d = \pi \frac{2n+1}{N/2-1}$  from the condition for  $\phi_d$  with  $N_e = N/2 - 1$ . We find this behaviour in Fig. 3: for the top figure there will be  $N_e + 1 = 3$  electrons in each leg, leading to a dip at  $\phi = \pi/2$  and for the bottom figure there will be 4 electrons in each leg leading to a dip at  $\phi = \pi/3$ . When  $t_{\perp} \neq 0$ , we find that the dips remain and are quite robust, even for values of  $t_{\perp}/t_{\parallel}$  as high as 0.1.

For strongly coupled chains, *i.e.* with a large coupling between the legs,  $t_{\perp} \gg t_{\parallel}$ , the bands corresponding to each leg are very far apart in the non-interacting case and one might expect the reappearance of SCS. This is, in fact, the case as can be seen in Fig. 4, where we plot the transmittance for a ladder with several values of  $t_{\perp}$  and fillings.

For this case, the total number of electrons in the lower band corresponds to the total filling  $N$  (for a less than half filled band) and the transmittance will involve  $N_e = N - 1$  electrons. Hence, the dips will be found at the fluxes  $\phi_d = \pi \frac{2n+1}{N-1}$  as seen in Fig. 4 for large values of  $t_{\perp}/t_{\parallel}$ . For smaller values of  $t_{\perp}$ , we find a shift in the location of the minima and sometimes a splitting of the dips. We have understood this numerically for a smaller system by realizing that the dips correspond to certain level crossings which occur for particular values of the magnetic flux.<sup>30</sup>

For intermediate values of the perpendicular hopping the dips disappear. It is interesting to see that, for constant filling, we find dips at different values of the flux for weak and strong coupling. Finite  $J$  introduces an extra spin shuffling in the system, reducing the depth and shifting the position of the dips.

#### 4. Quantum Interference

We consider here an annular  $\pi$ -conjugated molecules with  $N$  sites, weakly connected to non-interacting leads in the A or B configurations (Fig. 1c). Now the interacting

Hamiltonian  $H_{\text{ring}}$  describes the isolated  $\pi$ -conjugated molecule, modelled by the PPP Hamiltonian,<sup>34</sup> with on-site energy given by a gate voltage  $V_g$ :

$$\begin{aligned}
 H_{\text{ring}} = & -eV_g \sum_{i=1,\sigma}^N c_{i\sigma}^\dagger c_{i\sigma} - t \sum_{\langle ij \rangle, \sigma} c_{i\sigma}^\dagger c_{j\sigma} + \sum_i U_i \left( n_{i\downarrow} - \frac{1}{2} \right) \left( n_{i\uparrow} - \frac{1}{2} \right) \\
 & + \sum_{i>j} V_{ij} (n_i - 1)(n_j - 1)
 \end{aligned} \tag{6}$$

where the operators  $c_{i\sigma}^\dagger$  ( $c_{i\sigma}$ ) create (annihilate) an electron of spin  $\sigma$  in the  $\pi$  orbital of the Carbon atom at site  $i$ ,  $n$  are the corresponding number operators and  $\langle \dots \rangle$  stands for bonded pairs of Carbon atoms. The intersite interaction potential  $V_{ij}$  is parametrized so as to interpolate between  $U$  and  $e^2/r_{ij}$  in the limit  $r_{ij} \rightarrow \infty$ .<sup>35</sup> In the Ohno interpolation,  $V_{ij}$  is given by

$$V_{ij} = U_i (1 + 0.6117 r_{ij}^2)^{-1/2} \tag{7}$$

where the distance  $r_{ij}$  is in  $\text{\AA}$ . The standard Hubbard parameter for  $sp^2$  Carbon is  $U_i = 11.26$  eV and hopping parameter  $t$  for  $r = 1.397$   $\text{\AA}$  is 2.4 eV,<sup>36</sup> and all energies are in eV.

For the isolated benzene molecule, which has translational symmetry, the allowed total momentum quantum numbers are  $k = 2r\pi/(4n + 2) = r\pi/(2n + 1)$ , with  $r$  an integer. For a two-terminal set up like the one considered here, wave functions travelling through both branches of the molecule will interfere producing different interference patterns depending on the positions of the leads. The phase difference will be momentum times the difference in the lengths of the two trajectories (in units of the C-C separation):  $\Delta\phi = k\Delta x$ . For leads in the ‘‘para’’ position,  $\Delta x = 0$  and the waves are in phase, interfering constructively (Fig. 1c, A configuration). However, in the ‘‘meta’’ (B configuration) position ( $\Delta x = 2$ ), the interference will depend on the  $k$  value of the particular channel. For the highest occupied molecular orbital (HOMO) and lowest unoccupied molecular orbital (LUMO) the phase differences will be  $\Delta\phi = 2\pi/3$  and  $\Delta\phi = 4\pi/3$  respectively and the interference will reduce the amplitude in these channels.

In Fig. 5 we show results for the conductance through benzene molecules in the ‘‘para’’ and ‘‘meta’’ configurations of the leads. The nearly destructive interference effect for the latter case is clearly visible.

In view of the reduction of the HOMO (or LUMO) peaks for the ‘‘meta’’ configuration, one can ask whether disrupting translational invariance would lead to a larger conductance. This question was first addressed in Ref. 14 by introducing a local energy ( $\Sigma$ ) at one site in benzene, the real part of which would produce elastic scattering and its imaginary part, decoherence. These authors focused on the Fermi energy of the leads (set to zero) where the observed effect is small. In 37 we studied the effect of external perturbations on the main transmittance channels such as the HOMO and LUMO and we found a much larger response. These results are shown in the bottom part of Fig. 5, where an additional diagonal energy is added to the



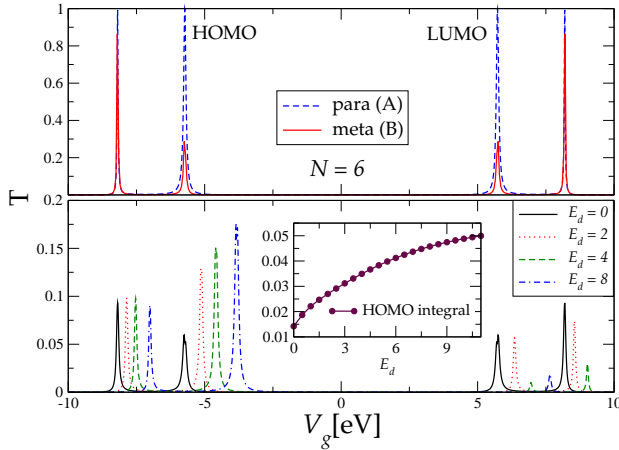


Fig. 5. Top: Transmittance vs. gate voltage (measured from the Fermi energy) through a benzene molecule for the “para” (A substitution in Fig. 1c) and “meta” (B substitution in Fig. 1c) configurations for  $t' = 0.4$  and a finite Lorentzian width  $\eta = 0.03$ . Bottom: Same for the “meta” configuration in the presence of different on-site potentials which break the translational invariance. Inset: evolution of the weight of the transmission peak through the HOMO as a function of the on-site potential.

site to the right of the B (“meta”) position (the effect is not qualitatively dependent on this position). It is clearly seen that, in this case, the small peak corresponding to the HOMO level develops and grows as the local energy is increased, disrupting the translational symmetry responsible for the destructive interference (see inset). We also find that this effect is much more striking for larger annulenes. These results are not affected by molecular vibrations at room temperature since modes that can cause decoherence are excited at temperatures higher than  $500K$ .<sup>14</sup>

## 5. Conclusion

We have reviewed results on the existence of dips in the conductance through finite strongly correlated low-dimensional systems which arise as a consequence of non-trivial destructive interference effects at fractional values of the flux quantum  $\Phi_0$ . This feature is a strong indication of the existence of SCS in these systems. We have presented results for the transmittance through interacting one-dimensional and anisotropic ladder rings. In all cases the dip structure is robust against finite interactions (small  $J$ 's or large  $U$  for the  $t - J$  or Hubbard models respectively). However, we find new dips and shifts of their positions with respect to the ideal scenario of complete charge-spin separation. We also find that the dip structure, originally predicted for 1D systems, is still present for two transmission channels modelled by a ladder system in the anisotropic limit. For a wide range of parameters, in particular for weak and strong hoppings across the rungs  $t_{\perp}$ , the dips remain,

but they disappear for intermediate values of this parameter. These findings open the possibility of measuring this peculiar phenomenon in real nanoscopic systems or artificial structures, such as rings of quantum dots on the sub- $\mu\text{m}$  scale, where the magnetic fields needed for this kind of experiments become accessible.

In addition, we have analyzed the resonant conductance through the HOMO and LUMO channels of benzene in the weak lead-molecule coupling regime. We find a strong dependence on the source-drain configuration and on the molecular geometry due to quantum interference.

## Acknowledgments

This investigation was sponsored by PIP 5254 of CONICET and PICT 2006/483 of the ANPCyT. We are partially supported by CONICET.

## References

1. D. Goldhaber-Gordon, H. Shtrikman, D. Mahalu, D. Abusch-Magder, U. Meirav, and M.A. Kastner, *Nature* **391**, 156 (1998).
2. S. M. Cronenwet, T. H. Oosterkamp, and L. P. Kouwenhoven, *Science* **281**, 540 (1998).
3. W.G. van der Wiel, S. De Franceschi, T. Fujisawa, J.M. Elzerman, S. Tarucha and L.P. Kouwenhoven, *Science* **289**, 2105 (2000).
4. Y. Oreg and D. Goldhaber-Gordon, *Phys. Rev. Lett.* **90**, 136602 (2003).
5. R. Žitko and J. Bonča, *Phys. Rev. B* **74**, 224411 (2006).
6. A. A. Aligia, K. Hallberg, B. Normand, and A. P. Kampf, *Phys. Rev. Lett.* **93**, 076801 (2004).
7. G. B. Martins, C. A. Bsser, K. A. Al-Hassanieh, A. Moreo, and E. Dagotto, *Phys. Rev. Lett.* **94**, 026804 (2005).
8. L. P. Kouwenhoven, F. W. J. Hekking, B. J. van Wees, C. J. P. M. Harmans, C. E. Timmering and C. T. Foxon, *Phys. Rev. Lett.* **65**, 361 (1990).
9. A. Aviram, M. A. Ratner, *Chem. Phys. Lett.* **29**, 277 (1974).
10. M. A. Reed, M. A. Reed, C. Zhou, C. J. Muller, T. P. Burgin, J. M. Tour, *Science* **278**, 252 (1997).
11. G. Cuniberti, G. Fagas, K. Richter (eds), *Introducing Molecular Electronics*, Springer, Berlin **2005**.
12. A. Nitzan, M. A. Ratner, *Science* **300**, 1384 (2003).
13. N. Tao, *Nature Nanotech.* **1**, 173-181 (2006).
14. D. Cardamone, C. Stafford, S. Mazumdar, *Nano Lett.* **6**, 2422 (2006).
15. S-H. Ke, W. Yang, H. Baranger, *Nano Lett.* **8**, 3257 (2008).
16. S. Yeganeh, M. Ratner, M. Galperin, A. Nitzan, *Nano Lett.* **9**, 1770 (2009).
17. J. Park, J.Park, A.N.Pasupathy, J.I.Goldsmith, C.Chang, Y.Yaish, J.R.Petta, M.Rinkoski, J.P.Sethna, H.D.Abruna, P.L.McEuen and D.C.Ralph, *Nature* **417**, 722-725 (2002).
18. L. Venkataraman, J. E. Klare, C. Nuckolls, M. S. Hybertsen and M. L. Steigerwald, *Nature* **442**, 904 (2006).
19. A. V. Danilov, S. Kubatkin, S. Kafanov, P. Hedegard, N. Stuhr-Hansen, K. Moth-Poulsen, and T. Bjornholm, *Nano Lett.* **8**, 1 (2008).
20. T. Dadoosh, T. Dadoosh, Y. Gordin, R. Krahne, I. Khivrich, D. Mahalu, V. Freydmann, J. Sperling, A. Yacoby, I. Bar, *Nature* **436**, 677 (2005).
21. E. A. Jagla, K. Hallberg, and C. A. Balseiro, *Phys. Rev. B* **47**, 5849 (1993).

22. C. Kollath, U. Schollwoeck and W. Zwerger, *Phys. Rev. Lett.* **95**, 176401 (2005)
23. S. White, *Phys. Rev. Lett.* **69**, 2863 (1992); K. Hallberg, *New Trends in Density Matrix Renormalization*, *Adv. in Phys.* **55**, 477 (2006); U. Schollwck, *The density-matrix renormalization group*, *Rev. Mod. Phys.* **77**, 259 (2005)
24. E. A. Jagla and C. A. Balseiro, *Phys. Rev. Lett.* **70**, 639 (1993).
25. S. Friederich and V. Meden, *Phys. Rev. B* **77**, 195122 (2008).
26. K. Hallberg, A. A. Aligia, A. Kampf and B. Normand, *Phys. Rev. Lett.* **93**, 067203 (2004).
27. J. Rincón, A. A. Aligia and K. Hallberg, *Phys. Rev. B* **79**, 035112 (2009).
28. J. Rincón, A. A. Aligia and K. Hallberg, *Physica B* **404**, 2270 (2009).
29. J. Rincón, K. Hallberg, and A. Aligia, *Physica B* **404**, 3147 (2009).
30. J. Rincón, K. Hallberg and A. A. Aligia, *Phys. Rev. B* **78**, 125115 (2008).
31. E. R. Davidson, *J. Comput. Phys.* **17**, (1975) 87; *Comput. Phys. Comm.* **53**, 49 (1989).
32. M. Ogata and H. Shiba, *Phys. Rev. B* **41**, 2326 (1990).
33. W. Caspers and P. Ilske, *Physica A* **157**, 1033 (1989); A. Schadschneider, *Phys. Rev. B* **51**, 10386 (1995).
34. R. Pariser, R. Parr, *J. Chem. Phys.* **21**, 466 (1953); J. A. Pople, *Trans. of the Faraday Soc.*, **49**, 1375 (1953).
35. K. Ohno, *Theor. Chim. Acta* **2**, 219 (1964).
36. Z. G. Soos, and S. Ramasesha, *Phys. Rev. B* **29**, 5410 (1984).
37. J. Rincón, K. Hallberg and S. Ramasesha, *Phys. Rev. Lett.* in print (2009).